

1 Exploring an approximation for the homogeneous freezing temperature of water
2 droplets

3

4

5 Kuan-Ting O¹, Robert Wood¹

6 [1] University of Washington, Department of Atmospheric Sciences, Seattle, WA,
7 USA

8

9

10

11

12

13

14

15

16

17

18

19

20

21

22

23

24

25

26

27 Corresponding author:

28 Kuan-Ting O

29 408 Atmospheric Sciences–Geophysics (ATG) Building

30 Box 351640, Seattle, Washington 98195-1640

31 Phone (206) 543-4250 | Fax (206) 543-0308

32 ktoandy@u.washington.edu

33 **Abstract**

34 In this work, based on the well-known formulae of classical nucleation theory
35 (CNT), the temperature $T_{N_c=1}$ at which the mean number of critical embryos inside a
36 droplet is unity is derived from the Boltzmann distribution function and explored as
37 an approximation for homogeneous freezing temperature of water droplets. Without
38 including the information of the applied cooling rate $\gamma_{cooling}$ and the number of
39 observed droplets $N_{total_droplets}$ in the calculation, the approximation $T_{N_c=1}$ is able to
40 reproduce the dependence of homogeneous freezing temperature on drop size V and
41 water activity a_w of aqueous drops observed in a wide range of experimental studies
42 for droplet diameter $> 10 \mu\text{m}$ and $a_w > 0.85$, suggesting the effect of $\gamma_{cooling}$ and
43 $N_{total_droplets}$ may be secondary compared to the effect of V and a_w on
44 homogeneous freezing temperatures in these size and water activity ranges under
45 realistic atmospheric conditions. We use the $T_{N_c=1}$ approximation to argue that the
46 distribution of homogeneous freezing temperatures observed in the experiments may
47 be partly explained by the spread in the size distribution of droplets used in the
48 particular experiment. It thus appears that the simplicity of this approximation makes
49 it potentially useful for predicting homogeneous freezing temperatures of water
50 droplets in the atmosphere.

51

52

53

54

55 Keywords: classical nucleation theory, homogeneous ice nucleation, freezing
56 temperature

57 **1. Introduction**

58 Since the summary article of McDonald (1953), it has been widely observed that
59 ice nucleation of water droplets does not occur at the ice melting temperature (e.g.
60 273.15 K at 1atm), and liquid water is frequently observed in clouds as cold as to 238
61 K (Rosenfeld and Woodley, 2000; Hu et al., 2010). Laboratory observations of
62 homogeneous ice nucleation in pure water generally show that all droplets do not
63 freeze at exactly the same temperature, and that the fraction of droplets that freeze in
64 a given time is a function of temperature and time (hereafter we refer to this type of
65 experiment as a *fraction experiment*) (e.g. Bigg 1953; Carte 1956; Broto and Clause,
66 1976; Earle et al., 2010; Riechers et al., 2013). Here, experimental data of the freezing
67 temperatures of pure water droplets from 15 independent studies over the past 60
68 years are collected (Fig. 1 and Table 1), showing a clear dependence of freezing
69 temperature upon drop volume across different experiments. Over the investigated
70 size interval (1-1000 μm diameter), observed freezing temperatures range from 232 K
71 to 240 K. The range of freezing temperatures and the volume dependence in Fig. 1 are
72 consistent with the experimental data reviewed in Pruppacher (1995).

73 On the other hand, solutes, at sufficiently high concentrations, can suppress the
74 homogeneous freezing temperature of water droplets. Koop et al. (2000) showed that
75 the depression of freezing temperature strongly depends on the water activity a_w of
76 the solution droplet, which has been confirmed in several independent experimental
77 studies (e.g. Knopf and Lopez, 2009; Knopf and Rigg, 2011). In this paper, two
78 aforementioned features of homogeneous ice nucleation observed in the experimental
79 data are examined – (1) the volume and water activity dependence of homogeneous

80 freezing temperatures of water droplets $T_f(V, a_w)$; (2) the distribution of
81 homogeneous freezing temperatures observed in fraction experiments $f(T_f)$. In this
82 paper, we describe only volume-based nucleation and do not include the droplet
83 surface effects on homogeneous ice nucleation as there remains considerable
84 uncertainty about the importance of surface nucleation (Kay et al., 2003; Duft and
85 Leisner, 2004). The unified explanations of the observed dependencies of the
86 homogeneous freezing temperature on droplet size and water activity have been
87 proposed by several studies based on different theoretical frameworks such as ice
88 nucleation rate J and density fluctuation (e.g. Pruppacher 1995; Baker and Baker
89 2004; Khvorostyanov and Curry 2009; Barahona 2014). In our study, based on a
90 cornerstone of classical nucleation theory (CNT), namely that a critical embryo
91 existing in a droplet triggers ice crystal formation, we explore a simple approximation
92 for the homogeneous freezing temperature, and seek a simpler parameterization to
93 describe homogeneous ice nucleation process in the atmosphere. Section 2 describes
94 the approximation; Section 3 gives the comparisons between the theoretical estimates
95 and the experimental data; Section 4 is the discussion; Section 5 is the summary.

96

97

98

99

100

101

102

103 2. Background

104 2.1 The approximation $T_{N_c=1}(V, a_w)$

105 According to CNT, the formation of a critical embryo inside a droplet can trigger
106 the freezing process in the droplet. The critical embryo defined as the i -mers having
107 the highest formation energy is formed by the critical fluctuation in orientation of
108 hydrogen bonds (e.g. density fluctuation) (Baker and Baker 2004), which is large
109 enough to provide the formation energy of the critical embryo $\Delta F_c(T, a_w)$ and
110 remove metastability of supercooled water. The probability of occurrence of the
111 critical fluctuation is $\exp(\frac{-\Delta F_c(T, a_w)}{k_B T})$ (Landau and Lifshitz, 1969, P.472-473;
112 Pruppacher and Klett, 1997), and thus the *mean number* of the critical embryos inside
113 a water droplet in thermal equilibrium can be predicted by a Boltzmann distribution
114 (Landau and Lifshitz, 1969, P.107; Vali, 1999),

$$115 N_{c_mean}(V, a_w, T) = V\rho \exp(\frac{-\Delta F_c(T, a_w)}{k_B T}) \quad (1)$$

116 where V is the volume of the droplet, ρ is the number density of water molecules,
117 k_B is Boltzmann's constant, T is the temperature of the droplet, and $\Delta F_c(T, a_w)$ is
118 the formation energy of the critical embryo in the droplet with water activity a_w at
119 T , which will be discussed in detail in Sect. 2.2. The Boltzmann distribution form of
120 the critical embryo is derived from the partitioning function of the grand canonical
121 ensemble, and it should be noted that the derived particle number of the Boltzmann
122 distribution function is not a "constant" but is a "mean" number (detailed derivation
123 and explanations can be found in Landau and Lifshitz, 1969, P.107 and Sadovskii,
124 2012, Chapter 3.1).

125 The total freezing time $\tau_{freezing}$ of a water droplet can be split conceptually into
 126 three stages – (1) $\tau_{meta_remove} (\sim \frac{1}{J})$ the time needed for the occurrence of the critical
 127 fluctuation (2) $\tau_{formation}$ the time needed to form a critical embryo and (3) $\tau_{growing}$
 128 the growing time for the critical embryo expanding to the whole droplet body. These
 129 depend on V , a_w and T of the droplet (Pruppacher and Klett 1997; Bauerecker et
 130 al., 2008). To observe freezing of droplets with volume V and water activity a_w
 131 occurring at temperature T , the residence time of freezing experiments $\tau_{residence}$ at
 132 T has to be longer than $\tau_{freezing}(V, a_w, T)$, resulting in a dependence of the
 133 homogeneous freezing temperature on the cooling rate $\gamma_{cooling}$ of droplets in principle.
 134 According to the theoretical estimates (see Pruppacher and Klett 1997, P.678), the
 135 time scale of $\tau_{formation} + \tau_{growing}$ for the size of the droplets investigated here is short
 136 compared with the typical residence times in the laboratory studies. Thus, the
 137 dominant factor determining the homogeneous freezing temperatures is τ_{meta_remove} .
 138 Because τ_{meta_remove} is the time needed for the occurrence of the critical fluctuation
 139 among water molecules, τ_{meta_remove} is shorter in a larger droplet with more
 140 molecules $V\rho$ or at lower temperature when the fluctuation probability
 141 $\exp(\frac{-\Delta F_c(T, a_w)}{k_B T})$ is higher; $\tau_{meta_remove}^{-1} \propto N_{c_mean}(V, a_w, T)$. Embryo interaction is a
 142 stochastic process and $N_{c_mean}(V, a_w, T)$ simply expresses the mean state, so there is
 143 always a spread of τ_{meta_remove} among droplets even in a idealized case that all the
 144 droplets used in the experiment have exactly the same V and a_w and are at exactly
 145 the same temperature T . The spread of τ_{meta_remove} can be wider when there are
 146 more observed droplets $N_{total_droplets}$, which in principle can explain the fraction

147 experiments that some droplets with shorter τ_{meta_remove} can always be frozen at
148 higher temperature, or in shorter time for droplets at the same temperature even when
149 the droplets have a monodisperse size distribution and exactly same a_w . Hereafter we
150 refer the distribution of homogeneous freezing temperatures owing to $N_{total_droplets}$
151 when all the droplets have exactly same V and a_w as a *stochastic feature*. Based
152 on above-mentioned principles, the homogenous freezing temperature of water
153 droplets and τ_{meta_remove} can each be written as a function of V , a_w , $\gamma_{cooling}$ and
154 $N_{total_droplets}$, namely $T_f(V, a_w, \gamma_{cooling}, N_{total_droplets})$ and
155 $\tau_{meta_remove}(V, a_w, \gamma_{cooling}, N_{total_droplets})$.

156 Koop et al. (1998) reported that observed homogeneous freezing temperatures do
157 not significantly depend on $\gamma_{cooling}$ of the droplets for $\gamma_{cooling}$ smaller than 20 K min^{-1}
158 (corresponding to vertical velocities 33.3 m s^{-1} in clear air). The results of Koop et al.
159 (1998) actually indicate that the slope of $\frac{\partial \tau_{meta_remove}}{\partial T}$ is very steep at the temperature
160 when the scale of τ_{meta_remove} is close to $\tau_{residence}$ in most practical experiments and
161 realistic atmospheric conditions, resulting in the small dependence of T_f on $\gamma_{cooling}$
162 as suggested by Brewer and Palmer (1951). Based on that, in most of the practical
163 freezing experiments and realistic atmospheric conditions ($\gamma_{cooling} < 20 \text{ K min}^{-1}$), the
164 observed homogeneous freezing temperatures can be considered as a threshold
165 temperature when $\frac{\partial \tau_{meta_remove}}{\partial T} \rightarrow \infty$. In this study, we intend to find this threshold
166 temperature directly from the information given by $N_{c_mean}(V, a_w, T)$. The number of
167 critical embryos derived from the Boltzmann distribution is a mean value and does
168 not provide any information regarding freezing time, so it can not be used to study the

169 dependence of the homogeneous freezing temperature on cooling rate (i.e. time
 170 dependence) and number of droplets used in the experiments (i.e. stochastic feature).
 171 Nevertheless, since the formation of one critical embryo is required to trigger the ice
 172 nucleation process in a droplet, $T_{N_c=1}$ may be a good approximation for the threshold
 173 temperature, the temperature at which the mean number of the critical embryos inside
 174 a droplet is unity, which can be given by

$$175 \quad N_{c_mean} = 1 = V\rho \exp\left(\frac{-\Delta F_c(T_{N_c=1}, a_w)}{k_B T_{N_c=1}}\right) \quad (2)$$

176 According to the formula of $\Delta F_c(T, a_w)$, $T_{N_c=1}$ is determined by V and a_w of
 177 the droplet, namely $T_{N_c=1}(V, a_w)$. Figure 2 shows the mean number of critical
 178 embryos inside a pure water droplet ($a_w = 1$) at different temperatures using Eq. (1)
 179 (see next section for details of $\Delta F_c(T, a_w)$ used in the calculation). It indicates that
 180 smaller droplets require lower temperatures to reach the state that $N_{c_mean} = 1$,
 181 showing the volume dependence of $T_{N_c=1}(V, a_w)$. Figure 3 shows the mean number of
 182 critical embryos inside a solution droplet with different values of water activity. The
 183 result indicates that more concentrated solution droplets (lower a_w) need lower
 184 temperature to reach the state that $N_{c_mean} = 1$. This represents the solution effect on
 185 $T_{N_c=1}(V, a_w)$. The sensitivity of $T_{N_c=1}(V, a_w)$ to the variation of diameter δd and
 186 water activity δa_w of droplets can be written as

$$187 \quad \delta T_{N_c=1} = \frac{\partial T_{N_c=1}}{\partial a_w} \delta a_w + \frac{\partial T_{N_c=1}}{\partial \log_{10} d} \delta \log_{10} d \quad (3)$$

188 where d is the diameter of droplet (μm). As shown in Fig. 1, the dependence of
 189 $T_{N_c=1}$ on $\log_{10} d$ is nearly linear, so the decadal log is used here to simply derive the

190 linear dependence. The values of $\frac{\partial T_{N_c=1}}{\partial a_w}$ and $\frac{\partial T_{N_c=1}}{\partial \log_{10} d}$ are about 216 K and 2.5 K
 191 respectively over the investigated interval of water activity and drop size, which are
 192 derived numerically from Eq. (2).

193 2.2 Formation energy of the critical embryo $\Delta F_c(T, a_w)$

194 The formation energy of the critical embryo $\Delta F_c(T, a_w)$ can be written as

$$195 \Delta F_c = \frac{1}{3} s \sigma_{i/w}(T, a_w) r_c^2 \quad (4)$$

$$196 r_c = \frac{2\sigma_{i/w}(T, a_w)v_1^{water}}{k_B T \ln\left(\frac{e_{sw}a_w}{e_{si}}\right) + k_B T \ln(a_w)} \quad (5)$$

197 where $\sigma_{i/w}(T, a_w)$ is the interfacial energy between liquid water and solid ice, s is
 198 the shape factor of the embryo (~ 21 by assuming the shape is hexagonal prism), r_c
 199 is the radius of the critical embryo, v_1^{water} is the volume of single water molecule,
 200 e_{sw} and e_{si} are the saturation vapor pressures over water and ice respectively
 201 (Murphy and Koop, 2005), and a_w is the water activity of the solution droplet (see
 202 detailed derivations of Eq. (4) in Defour and Defay, 1963 and Pruppacher and Klett,
 203 1997). It should be noted that the term $k_B T \ln(a_w)$ in r_c (Eq. (5)) is the *entropy of*
 204 *unmixing* which originates from the change of the Gibbs free energy of the bulk
 205 solution during freezing, and is usually neglected in the previous theoretical studies
 206 (Bourne and Davey, 1976; Black 2007). Barahona (2014) pointed out that although
 207 this term is small for dilute solution, it should not be neglected when applying to high
 208 concentration solution droplets (see Eq. (8) in Barahona (2014)).

209 The value of interfacial energy between liquid water and solid ice $\sigma_{i/w}(T, a_w)$ is
 210 needed for our calculation of Eq. (4) and (5). As most studies suggest that the

211 temperature dependence of $\sigma_{i/w}(T, a_w)$ should be linear (Ickes et al., 2015), and that
 212 increasing the concentration of the solution droplet increases the value of $\sigma_{i/w}(T, a_w)$
 213 (Jones and Chadwick, 1971; Alpert et al. 2011), $\sigma_{i/w}(T, a_w)$ can be written as

$$214 \quad \sigma_{i/w}(T, a_w) = \sigma_{i/w,e} + \frac{\partial \sigma_{i/w}}{\partial T}(T - T_0) + \frac{\partial \sigma_{i/w}}{\partial a_w}(1 - a_w) \quad (6)$$

215 where $\sigma_{i/w,e}$ is the interfacial energy at the equilibrium temperature of pure ice-water,
 216 and T_0 is the equilibrium temperature. The direct measurement of $\sigma_{i/w}(T, a_w)$ is
 217 extremely difficult, so most of the estimations are based on combinations of CNT and
 218 laboratory measurements of T_f and observed freezing rate to retrieve the values of
 219 $\sigma_{i/w}(T, a_w)$ (e.g. Zobrist et al., 2007; Murray et al., 2010). These studies have shown
 220 considerable diversity in the reported estimations of $\sigma_{i/w}(T, a_w)$ (Ickes et al., 2015).

221 Instead, we use values of $\sigma_{i/w,e}$ and $\frac{\partial \sigma_{i/w}}{\partial T}$ derived from a state-of-the-art molecular
 222 dynamics model that explicitly simulates the molecular configurations under
 223 supercooling conditions. Benet et al. (2014) gives values of $\sigma_{i/w,e}$ from the TIP4P
 224 water model ($\sigma_{i/w,e} = 26.5 \times 10^{-3} \text{ J m}^{-2}$), TIP4P/2005 water model ($\sigma_{i/w,e} = 27 \times 10^{-3} \text{ J m}^{-2}$),
 225 and TIP4P-Ew water model ($\sigma_{i/w,e} = 27.5 \times 10^{-3} \text{ J m}^{-2}$), and these three values will all be
 226 used in our calculations. According to Ickes et al. (2015), the values of $\sigma_{i/w,e}$ used
 227 here are about the median of all the values derived from the previous studies.

228 Regarding $\frac{\partial \sigma_{i/w}}{\partial T}$, Espinosa et al. (2014) provided an average value of $0.25 \times 10^{-3} \text{ (J}$
 229 $\text{ m}^{-2} \text{ K}^{-1})$ from three different water molecular models (TIP4P/ICE, TIP4P and
 230 TIP4P/2005) down to a supercooling of about 30K. Regarding $\frac{\partial \sigma_{i/w}}{\partial a_w}$, Barahona
 231 (2014) proposed a new thermodynamic framework approximating the interfacial
 232 energy of ice-solution by assuming the interface between solid ice and liquid water is

233 made of liquid molecules trapped by the solid matrix, which gives the relationship
 234 between $\sigma_{i/w}$ and a_w . Based on this approximation, the solution effect on the
 235 interfacial energy can be written as

$$236 \quad \frac{\partial \sigma_{i/w}}{\partial a_w} = - \frac{\Gamma_w^2 s_{area} k_B T \frac{1}{a_w}}{(36\pi(v_1^{water})^2)^{1/3}} \quad (7)$$

237 where Γ_w is the surface excess of water (~ 1.46) (Spaepen 1975) and s_{area} is the
 238 surface area parameter ($\sim 1.105 \text{ mol}^{2/3}$) (see Barahona 2014 for details). The values of
 239 $\sigma_{i/w}(T, a_w)$ estimated from above studies are used to derive the numerical result
 240 $T_{N_c=1}(V, a_w)$ presented here.

241 **3. Results – Comparison between the approximation and the experimental data**

242 **3.1 Volume and water activity dependence of $T_f(V, a_w)$**

243 To test our approximation, we aim to compare the observed $T_f(V, a_w)$ and
 244 $f(T_f)$ with $T_{N_c=1}(V, a_w)$ derived using the constraint in Eq. (2). First,
 245 $T_{N_c=1}(V, a_w = 1)$ of pure water droplet is derived. Figure 1 shows the comparison
 246 between the experimentally determined homogeneous freezing temperatures
 247 $T_f(V, a_w = 1)$ (details of the experiments are provided in Table 1) and the
 248 approximations $T_{N_c=1}(V, a_w = 1)$. For droplet diameters $> 10\mu\text{m}$, the theoretical values
 249 of $T_{N_c=1}(V, a_w = 1)$ derived by the value of $\sigma_{i/w,e}$ from TIP4P water model agree
 250 very well with most of the experimental data $T_f(V, a_w = 1)$. Using the values of $\sigma_{i/w,e}$
 251 from TIP4P/2005 and TIP4P-Ew leads to a shift downward of about 1~2 K of
 252 $T_{N_c=1}(V, a_w = 1)$. There is one study regarding the time dependence should be
 253 mentioned. The laboratory observation of Murray et al. (2010) (black triangle in Fig.
 254 1) showed that varying of cooling rate from 2.5 K min^{-1} to 10 K min^{-1} corresponds to a

255 shift of 0.5 K to 1 K in observed freezing temperatures of pure water droplets, and our
 256 best agreement estimates $T_{N_c=1}(V, a_w = 1)$ can only explain the experimental data with
 257 slowest cooling rate (2.5 K min^{-1}). The finding of Murray et al. (2010) will be
 258 discussed in Sect. 4. For droplets smaller than $10 \text{ }\mu\text{m}$ (diameter), there are obvious
 259 deviations of observed freezing temperatures among the experimental studies. These
 260 studies do not provide enough information regarding $\gamma_{cooling}$, $N_{total_droplets}$ and the
 261 spread in drop size, so we cannot evaluate what causes the disparity. We suggest that
 262 freezing experiments of pure droplets smaller than $10 \text{ }\mu\text{m}$ (diameter) need more
 263 refinement and should report the potentially important dependencies such as applied
 264 cooling rate, size distribution of droplets and number of observed droplets used in
 265 experiments.

266 Second, the solution effect on homogeneous freezing temperature $T_f(V, a_w)$ is
 267 explored by changing the water activity in Eq. (5) and (6) to derive the approximation
 268 $T_{N_c=1}(V, a_w)$, which will be compared with the experimental data collected in Koop et
 269 al. (2000), Knopf and Lopez (2009) and Knopf and Rigg (2011). Size of the droplets
 270 used in the collected experimental data ranges from $1\mu\text{m}$ to $10 \text{ }\mu\text{m}$ in Koop et al.
 271 (2000), from $10\mu\text{m}$ to $80\mu\text{m}$ in Knopf and Lopez (2009) and from $20\mu\text{m}$ to $80\mu\text{m}$ in
 272 Knopf and Rigg (2011), and these sizes are included to calculate the approximation
 273 $T_{N_c=1}(V, a_w)$. Figure 4 shows the comparison between the experimental data and the
 274 approximation $T_{N_c=1}(V, a_w)$. Without considering the time dependence ($\gamma_{cooling}$
 275 varying from 1 K min^{-1} to 10 K min^{-1} among all the experiments) and the stochastic
 276 feature (i.e. $N_{total_droplets}$), the result shows that the approximation $T_{N_c=1}(V, a_w)$ is in
 277 good agreement with the experimental data for $a_w > 0.85$. The scattering of the

278 experimental data between the theoretical estimates for $a_w > 0.85$ (i.e. $T_{N_c=1}$ for
279 $d=1$ to $80 \mu\text{m}$) suggests that the spread of droplet size applied in the experiments
280 may play an important role in the spread of homogeneous freezing temperatures. For
281 the solution droplets with high concentration ($a_w < 0.85$), the observed freezing
282 temperatures show considerable spread. Abbatt et al. (2006) suggests that the
283 disparity of the experimental data for low a_w can be partly attributed to a variety of
284 heterogeneous process, which can result in the higher observed freezing temperatures.
285 In addition, as suggested by Knopf and Lopez (2009), the deviations at low water
286 activity may be most likely due to our incomplete understanding of a_w for certain
287 aqueous solutions and the corresponding uncertainties. Future experimental study is
288 suggested to focus on the freezing process of solution droplets with high solute
289 concentration ($a_w < 0.85$) to clarify the causes of the disparity.

290 Regarding the experimental uncertainty, Knopf and Lopez (2009) reported that
291 the value of a_w for supercooled aqueous solutions has the experimental uncertainty
292 δa_w of about ± 0.01 , which can result in the variation in $T_{N_c=1}$ of about ± 2 K based
293 on Eq. (3). Riechers et al. (2013) reported that the size of droplets produced by the
294 microfluidic device used in their experiment has three standard deviations (99.7%) of
295 about $18 \mu\text{m}$ to $33 \mu\text{m}$ in diameter, which can cause the variation in $T_{N_c=1}$ of about \pm
296 0.2 K to ± 0.5 K based on Eq. (3). Therefore, the variation in $T_{N_c=1}$ caused by the
297 experimental uncertainties δa_w and δd can be both substantial and should not be
298 neglected. We suggest future experimental studies should provide detailed
299 information regarding experimental uncertainties δa_w and δd for the purpose of
300 better constraining the observed freezing temperatures.

301 **3.2 Fraction of frozen pure water droplets as a function of temperature** $f(T_f)$

302 To further examine the application of $T_{N_c=1}(V, a_w)$ in homogeneous ice
303 nucleation, $T_{N_c=1}(V, a_w)$ is compared to the experimental data of the fraction
304 experiment of Riechers et al. (2013). According to CNT, the stochastic feature of the
305 ice nucleation process can basically explain the distribution of freezing temperatures
306 observed in the fraction experiment (Pruppacher and Klett, 1997, Eq. (7-71); Koop et
307 al., 1998; Niedermeier et al., 2011). However, current technology to produce water
308 droplets for such experiments introduces a spread of sizes, and the freezing
309 temperatures show a clear dependence on droplet volume (Fig. 1), so the spread in
310 sizes of water droplets used in the experiments may be important for explaining the
311 distribution $f(T_f)$. In other words, the size distribution of droplets used in a given
312 experiment may be an important factor governing the observed spread of freezing
313 temperatures (i.e. dotted line shown in Fig. 1). To test this, we incorporate the
314 reported droplet size distribution width into the numerical calculation. Unique among
315 such studies, Riechers et al. (2013) report both the spread of homogeneous freezing
316 temperatures and the mean μ and standard deviation σ of droplet size. According to
317 Eq. (3), the spread in the size distribution of water droplets will result in a spread in
318 the fraction of frozen droplets because larger droplets have higher $T_{N_c=1}(V, a_w)$ (i.e.
319 require less supercooling to freeze). Given the droplet size width, the distribution of
320 the approximations $T_{N_c=1}(V, a_w)$ of droplets can be derived from Eq. (2). Given a
321 Gaussian distribution of drop sizes, we estimate the fraction of drops that will freeze
322 at a given temperature *solely by assuming that the spread in freezing temperatures*
323 *arises from the spread in droplet sizes* based on Eq. (3). For example, we estimate

324 $T_{N_c=1}(V, a_w)$ of the droplets with size of $\mu+3\sigma$ (\sim the largest 0.15% of the drops) as
 325 the theoretical onset freezing temperature T_f^{onset} , $T_{N_c=1}(V, a_w)$ of the droplets with
 326 size of $\mu+1.64\sigma$ (\approx the largest 10% of the drops) as the theoretical estimates $T_f^{10\%}$,
 327 $T_{N_c=1}(V, a_w)$ of the droplets with mean size as the theoretical estimates $T_f^{50\%}$, and
 328 $T_{N_c=1}(V, a_w)$ of the droplets with size of $\mu-1.64\sigma$ (\approx the smallest 10% of the drops) as
 329 the theoretical estimates $T_f^{90\%}$, and $T_{N_c=1}(V, a_w)$ of the droplets with size of $\mu-3\sigma$ (\approx
 330 the smallest 0.15% of the drops) as the theoretical estimates T_f^{end} . The results
 331 presented in this section only use the value of $\sigma_{i/w,e}$ from the TIP4P water model,
 332 which has the best agreement with the experimental data shown in Sect. 3.1 (Fig. 1).

333 There are five experimental results from Riechers et al. (2013), each with
 334 different μ and σ . The comparisons (Fig. 5 and Table 2) show that our estimates
 335 match the experimental data fairly well. The slope of the freezing fraction versus
 336 temperature in the theoretical results is driven entirely by the reported spread in the
 337 size distribution of drops and matches fairly well with the observed slope, although
 338 across the experiments the theoretical slope is somewhat greater (observed values are
 339 shifted to the right of the blue curve at the higher temperatures but mostly to the left at
 340 the lower temperature), which might be attributable to the stochastic feature of the ice
 341 nucleation process. That said, the observational uncertainties in the experimental
 342 values of T_{on-set} , $T_{10\%}$, $T_{50\%}$ and $T_{90\%}$ more or less span the theoretical values
 343 derived from Eq. (2). Riechers et al. (2013) also reported that during cooling, the
 344 majority of the droplets are frozen over a temperature interval of 0.84-0.98 K, which
 345 is consistent with the range between the theoretical estimates T_f^{onset} and T_f^{end} derived
 346 here, namely 0.42-1.06 K from five different droplet size distributions, suggesting the

347 spread in droplet size (i.e. a disperse distribution) may be an important factor
348 governing the spread of the homogeneous freezing temperatures observed in a given
349 fraction experiment.

350 The comparison made in Sect. 3.1 to 3.2 shows that the distribution of the
351 freezing temperatures among the data can mostly be explained by the dependence of
352 $T_{N_c=1}(V, a_w)$ on V and a_w for droplet diameter $> 10 \mu\text{m}$ and $a_w > 0.85$ without
353 considering the dependence of homogeneous freezing temperature on $N_{total_droplets}$
354 and $\gamma_{cooling}$ in the calculations. It suggests that in most of the practical experiments
355 and for most atmospheric conditions, the time scale of $\tau_{residence}$ is shorter than
356 τ_{meta_remove} at the temperatures higher than $T_{N_c=1}(V, a_w)$ (i.e. $\tau_{residence} < \tau_{meta_remove}$,
357 when $T > T_{N_c=1}(V, a_w)$), and when the temperature of the droplets is close to
358 $T_{N_c=1}(V, a_w)$, the time scale of τ_{meta_remove} decreases strongly with temperature
359 decreases and becomes shorter than $\tau_{residence}$ of the experiments (i.e. $\tau_{residence} >$
360 τ_{meta_remove} when $T < T_{N_c=1}(V, a_w)$). This leads to the result that most of the
361 homogeneous ice nucleation process can only be observed at temperatures close to
362 $T_{N_c=1}(V, a_w)$ even though in principle, droplets can be frozen at any temperature.

363 4. Discussion

364 As mentioned in Sect. 2, the observed freezing temperatures with $\gamma_{cooling} \sim 2.5 \text{ K}$
365 min^{-1} reported in Murray et al. (2010) can be well described by $T_{N_c=1}(V, a_w)$, but it
366 also showed there is a shift of 0.5 K to 1 K in observed freezing temperatures when
367 varying the cooling rate from 2.5 K min^{-1} to 10 K min^{-1} . One possibility is that the
368 total freezing time $\tau_{freezing}$ needed to freeze a droplet at $T_{N_c=1}(V, a_w)$ is longer than

369 the time scale of $\tau_{residence}$ when $\gamma_{cooling}$ is higher than 2.5 K min^{-1} , which may be
 370 attributed to τ_{meta_remove} , $\tau_{formation}$ or $\tau_{growing}$. Without considering the experimental
 371 uncertainty associated with the thermal equilibrium time $\tau_{thermal}$, these 0.5K to 1K
 372 shifts corresponds to 3s to 6s shifts (for $\gamma_{cooling} = -10 \text{ K min}^{-1}$), which may be partly
 373 caused by $\tau_{formation} + \tau_{growing}$. Bauerecker et al. (2008) (hereafter Ba08) explored an
 374 advanced method providing time series of water droplet temperature during the entire
 375 cooling and freezing process (from supercooled water to completely freezing) using
 376 an infrared camera. The results of Ba08 showed that for the droplet sized 3mm
 377 (diameter), $\tau_{growing}$ is around 20s and $\tau_{thermal}$ is around 60s. The droplet used in
 378 Ba08 is much larger than the size normally used in the freezing experiments because
 379 of the limitation of IR camera sensitivity. If $\tau_{growing}$ linearly depends on drop radius,
 380 we may expect it to be several tenths of a second for the drops sized 10-100 μm in
 381 diameter. We suggest that the infrared camera technique should be used more widely
 382 in the future experimental studies of ice nucleation with smaller droplets, which can
 383 add significant insights into the time dependence study of ice nucleation, and clarify
 384 the importance of τ_{meta_remove} , $\tau_{formation}$ and $\tau_{growing}$ observed in the experiments. On
 385 the other hand, Koop et al. (1998) suggested that when the cooling rate is smaller than
 386 about 2 K min^{-1} , mass transport of water can take place between the frozen ice
 387 particles and supercooled droplets, but if the cooling rate is too large, it can cause an
 388 offset between the measured temperature and the actual temperature of the drops,
 389 which can both cause a bias of the observed freezing temperatures. Therefore, we
 390 suggest that in future experimental studies, in order to precisely measure $\frac{\partial T_f}{\partial \gamma_{cooling}}$,
 391 potential biases at high cooling rate and the shift caused by $\tau_{formation} + \tau_{growing}$ should

392 be better constrained. Since Koop et al. (1998) and Murray et al. (2010) showed
393 different dependencies of homogeneous freezing temperatures on $\gamma_{cooling}$, future
394 experiments should reexamine and perform the same experiments for $\gamma_{cooling} > 2.5$ K
395 min^{-1} . The results shown in Fig. 1 and Fig. 4 suggest that the time consideration may
396 be more important when droplet volume and water activity are low where the
397 experimental data show considerable inconsistency (i.e. $a_w < 0.85$ and $d < 10\mu\text{m}$),
398 and future experiments are suggested to emphasize these droplet size and water
399 activity ranges.

400 5. Summary

401 The limitation of our method proposed here is that the time dependence and the
402 stochastic feature of homogeneous freezing temperature cannot be considered because
403 the Boltzmann distribution applied here is a average distribution and does not provide
404 any information regarding time. Combining the well-known Boltzmann distribution
405 function for the mean number of critical embryos $N_{c_mean}(V, a_w, T)$ and their
406 formation energy $\Delta F_c(T, a_w)$ from CNT formulae, $T_{N_c=1}(V, a_w)$ is derived as a
407 function of volume and water activity of water droplets. With the comparison made in
408 Sect. 3.1 to 3.2, it can be summarized that under most atmospheric conditions,
409 homogeneous freezing temperatures can be well described by the new approximation
410 $T_{N_c=1}(V, a_w)$ proposed here without considering information of the applied cooling
411 rate (i.e. time dependence) and the number of droplets used in the experiment (i.e.
412 stochastic feature) for $d > 10\mu\text{m}$ and $a_w > 0.85$. Future experimental study is
413 suggested to focus on the homogeneous freezing process of droplets with high solute

414 concentration ($a_w < 0.85$) and small volume ($d < 10\mu\text{m}$). The experimental spread
415 in homogeneous freezing temperatures of water droplets may be partly explained by
416 the size distribution of droplets used in the experiments. The advantage of our
417 approximation in the cloud modeling is “the temperature history” of droplets is not
418 required to calculate the homogeneous freezing temperature as it is when using the ice
419 nucleation rate (i.e. Eq. (7-71) in Pruppacher and Klett, 1997). When using the ice
420 nucleation rate $J(T(t))$, the complete temperature history of droplets is needed to
421 calculate the integration of $J(T(t))$ with respect to time in order to consider the time
422 dependence and the stochastic feature, which can introduce considerable complexity
423 in cloud modeling. However, based on the experimental studies of homogeneous
424 freezing temperature collected and discussed in our study, we suggest in most of the
425 practical experiments and realistic atmospheric conditions (i.e. $\gamma_{cooling} < 20 \text{ K min}^{-1}$),
426 the time dependence and the stochastic feature of homogeneous freezing temperature
427 may be a secondary factor compared to the effect of volume and water activity for
428 droplet diameter $> 10 \mu\text{m}$ and $a_w > 0.85$. The approximation proposed here is
429 relatively simpler to be implemented into cloud models and may improve the
430 representation of homogeneous ice nucleation in the atmosphere.

431

432

433

434

435

436

437 **Acknowledgements**

438 **The authors gratefully appreciate helpful discussion with Marcia Baker, Daniel**
439 **Cziczo and Sarvesh Garimella who provided important insight and guidance for**
440 **this study. Two anonymous reviewers are thanked for providing important**
441 **feedback that helped to improve the paper. The authors thank Thomas Koop for**
442 **his help in supplying the data in Figure 4.**

443

444 **References**

445 Abbatt, J. P., Benz, S., Cziczo, D. J., Kanji, Z., Lohmann, U. and Mohler, O.: Solid
446 ammonium sulfate aerosols as ice nuclei: a pathway for cirrus cloud formation,
447 Science, 313, 1770-1773, 1129726 [pii], 2006.

448

449 Alpert, P. A., Aller, J. Y., and Knopf, D. A.: Initiation of the ice phase by marine
450 biogenic surfaces in supersaturated gas and supercooled aqueous phases, Phys. Chem.
451 Chem. Phys., 13, 19882–19894, 2011.

452 Baker, M. and Baker, M.: A new look at homogeneous freezing of water, Geophys.
453 Res. Lett., 31, L19102, doi:10.1029/2004GL020483, 2004.

454 Barahona, D.: Analysis of the effect of water activity on ice formation using a new
455 thermodynamic framework, Atmospheric Chemistry and Physics, 14, 7665-7680,
456 2014.

457

458 Bauerecker, S., Ulbig, P., Buch, V., Vrbka, L. and Jungwirth, P.: Monitoring ice
459 nucleation in pure and salty water via high-speed imaging and computer simulations,
460 The Journal of Physical Chemistry C, 112, 7631-7636, 2008.

461 Black, S.: Simulating nucleation of molecular solids, P. Roy. Soc. A, 463, 2799–2811,
462 2007.

463 Bourne, J. and Davey, R.: The role of solvent-solute interactions in determining
464 crystal growth mechanisms from solution: I. The surface entropy factor, J. Cryst.
465 Growth, 36, 278–286, 1976.

466 Benet, J., MacDowell, L. G. and Sanz, E.: A study of the ice–water interface using the
467 TIP4P/2005 water model, *Physical Chemistry Chemical Physics*, 16, 22159–22166,
468 2014.

469

470 Bertram, A. K., Koop, T., Molina, L. T. and Molina, M. J.: Ice formation in (NH₄)
471 2SO₄-H₂O particles, *The Journal of Physical Chemistry A*, 104, 584–588, 2000.

472

473 Bigg, E. K.: The supercooling of water, *Proc. Phys. Soc. B*, 66, 688– 694, doi:
474 10.1088/0370-1301/66/8/309, 1953.

475

476 Brewer, A. W. and Palmer, H. P.: Freezing of supercooled water, *Proc. Phys. Soc. B*,
477 64, 765–773, 1951.

478 Broto, F. and Clause, D.: A study of the freezing of supercooled water dispersed
479 within emulsions by differential scanning calorimetry, *J. Phys. C Solid State*, 9(23),
480 4251, doi: 10.1088/0022-3719/9/23/009, 1976.

481

482 Carte, A.: The freezing of water droplets, *Proc. Phys. Soc. B*, 69(10), 1028–1037,
483 1956.

484 Cziczo, D. and Abbatt, J.: Deliquescence, efflorescence, and supercooling of
485 ammonium sulfate aerosols at low temperature: Implications for cirrus cloud
486 formation and aerosol phase in the atmosphere, *Journal of Geophysical Research:*
487 *Atmospheres* (1984–2012), 104, 13781–13790, 1999.

488 Dufour, L. and Defay, R.: *Thermodynamics of clouds*, Academic Press, New York,
489 USA, 1963.

490 Duft, D. and Leisner, T.: Laboratory evidence for volume-dominated nucleation of ice
491 in supercooled water microdroplets, *Atmospheric Chemistry and Physics*, 4,
492 1997–2000, 2004.

493

494 Earle, M., Kuhn, T., Khalizov, A. and Sloan, J.: Volume nucleation rates for
495 homogeneous freezing in supercooled water microdroplets: results from a combined
496 experimental and modelling approach, *Atmospheric Chemistry and Physics*, 10,
497 7945–7961, 2010.

498 Espinosa, J., Sanz, E., Valeriani, C., and Vega, C.: Homogeneous ice nucleation
499 evaluated for several water models, *J. Chem. Phys.*, 141, 18C529, doi:
500 10.1063/1.4897524, 2014.

501 Hoffer, T. E.: A laboratory investigation of droplet freezing, *J. Meteorol.*, 18, 766-778,
502 1961.

503

504 Hu, Y., Rodier, S., Xu, K., Sun, W., Huang, J., Lin, B., Zhai, P., and Josset, D.:
505 Occurrence, liquid water content, and fraction of supercooled water clouds from
506 combined CALIOP/IIR/MODIS measurements, *J. Geophys. Res.-Atmos.*, 115(19),
507 doi: 10.1029/2009JD012384, 2010.

508 Ickes, L., Welti, A., Hoose, C., and Lohmann, U.: Classical nucleation theory of
509 homogeneous freezing of water: thermodynamic and kinetic parameters, *Phys. Chem.*
510 *Chem. Phys.*, 17, 5514-5537, 2015.

511 Jones, D. and Chadwick, G.: Experimental measurement of solid-liquid interfacial
512 energies: The ice-water-sodium chloride system, *J. Cryst. Growth*, 11, 260-264, 1971.

513

514 Kay, J., Tsemekhman, V., Larson, B., Baker, M. and Swanson, B.: Comment on
515 evidence for surface-initiated homogeneous nucleation, *Atmospheric Chemistry and*
516 *Physics*, 3, 1439-1443, 2003.

517

518 Khvorostyanov, V. I. and Curry, J. A.: Critical humidities of homogeneous and
519 heterogeneous ice nucleation: Inferences from extended classical nucleation theory,
520 *Journal of Geophysical Research: Atmospheres (1984–2012)*, 114(D4), 2009.

521

522 Knopf, D. A. and Lopez, M. D.: Homogeneous ice freezing temperatures and ice
523 nucleation rates of aqueous ammonium sulfate and aqueous levoglucosan particles for
524 relevant atmospheric conditions, *Physical Chemistry Chemical Physics*, 11,
525 8056-8068, 2009.

526

527 Knopf, D. A. and Rigg, Y. J.: Homogeneous ice nucleation from aqueous
528 inorganic/organic particles representative of biomass burning: Water activity, freezing
529 temperatures, nucleation rates, *J. Phys. Chem. A*, 115, 762–773, 2011.

530 Koop, T., Luo, B., Tsias, A. and Peter, T.: Water activity as the determinant for
531 homogeneous ice nucleation in aqueous solutions, *Nature*, 406, 611-614, 2000.
532

533 Koop, T., Ng, H. P., Molina, L. T. and Molina, M. J.: A new optical technique to
534 study aerosol phase transitions: The nucleation of ice from H₂SO₄ aerosols, *The*
535 *Journal of Physical Chemistry A*, 102, 8924-8931, 1998.
536

537 Kuhns, I. and Mason, B.: The supercooling and freezing of small water droplets
538 falling in air and other gases, *Proceedings of the Royal Society of London. Series*
539 *A. Mathematical and Physical Sciences*, 302, 437-452, 1968.
540

541 Landau, L. and Lifshitz, E.: *Statistical Physics: V. 5: Course of Theoretical Physics*,
542 Pergamon Press, 1969.
543

544 Langham, E. and Mason, B.: The heterogeneous and homogeneous nucleation of
545 supercooled water, *Proceedings of the Royal Society of London. Series*
546 *A. Mathematical and Physical Sciences*, 247, 493-504, 1958.
547

548 Larson, B. H. and Swanson, B. D.: Experimental investigation of the homogeneous
549 freezing of aqueous ammonium sulfate droplets, *The Journal of Physical Chemistry A*,
550 110, 1907-1916, 2006.
551

552 McDonald, J. E.: Homogeneous nucleation of supercooled water drops, *J. Meteorol.*,
553 10, 416-433, 1953.
554

555 Mossop, S.: The freezing of supercooled water, *P. Phys. Soc. Lond. B*, 68(4), 193, doi:
556 10.1088/0370-1301/68/4/301, 1955.

557 Murphy, D. and Koop, T.: Review of the vapour pressures of ice and supercooled
558 water for atmospheric applications, *Q. J. R. Meteorol. Soc.*, 131, 1539-1565, 2005.
559

560 Murray, B., Broadley, S., Wilson, T., Bull, S., Wills, R., Christenson, H. and Murray,
561 E.: Kinetics of the homogeneous freezing of water, *Physical Chemistry Chemical*
562 *Physics*, 12, 10380-10387, 2010.
563

564 Niedermeier, D., Shaw, R., Hartmann, S., Wex, H., Clauss, T., Voigtländer, J. and
565 Stratmann, F.: Heterogeneous ice nucleation: exploring the transition from stochastic
566 to singular freezing behavior, 11, 8767-8775, 2011.
567
568 Pound, G. M., Madonna, L. and Peake, S.: Critical supercooling of pure water
569 droplets by a new microscopic technique, J. Colloid Sci., 8, 187-193, 1953.
570
571 Prenni, A. J., Wise, M. E., Brooks, S. D. and Tolbert, M. A.: Ice nucleation in sulfuric
572 acid and ammonium sulfate particles, Journal of Geophysical Research: Atmospheres
573 (1984–2012), 106, 3037-3044, 2001.
574
575 Pruppacher, H. and Klett, J.: Microphysics of clouds and precipitation, 2nd Edn.,
576 Kluwer Academic Publishers, Boston, MA, 1997

577 Pruppacher, H.: A new look at homogeneous ice nucleation in supercooled water
578 drops, J. Atmos. Sci., 52, 1924-1933, 1995.
579
580 Riechers, B., Wittbracht, F., Hütten, A. and Koop, T.: The homogeneous ice
581 nucleation rate of water droplets produced in a microfluidic device and the role of
582 temperature uncertainty, Physical Chemistry Chemical Physics, 15, 5873-5887, 2013.
583
584 Rosenfeld, D., and Woodley, W. L.: Deep Convective Clouds with Sustained
585 Supercooled Liquid Water down to -37.5C. *Nature* 405, 440–42, 2000.
586
587 Sadvskii, M. V.: Statistical Physics. De Gruyter Studies in Mathematical Physics.
588 Berlin: De Gruyter, 2012.
589
590 Spaepen, F.: A structural model for the solid-liquid interface in monatomic systems,
591 Acta Metallurgica, 23, 729–743, 1975.

592
593 Stan, C. A., Schneider, G. F., Shevkoplyas, S. S., Hashimoto, M., Ibanescu, M., Wiley,
594 B. J. and Whitesides, G. M.: A microfluidic apparatus for the study of ice nucleation
595 in supercooled water drops, Lab on a Chip, 9, 2293-2305, 2009.
596

597 Vali, G.: Ice Nucleation-Theory: A Tutorial, Presented at the NCAR/ASP 1999
598 Summer Colloquium, 1999 (unpublished).

599

600 Zobrist, B., Koop, T., Luo, B., Marcolli, C., and Peter, T.: Heterogeneous ice
601 nucleation rate coefficient of water droplets coated by a nonadecanol monolayer, J.
602 Phys. Chem. C, 111, 2149–2155, 2007.

603

604

605

606

607

608

609

610

611

612

613

614

615

616

617

618

619

620

References	Diameter (μm)	T_f (K)	Diameter Range (μm)	Range of freezing temperatures (K)	Cooling rate	Uncertainty (K)
Pound et al. (1953)	30 ⁺	233.15 ^a	[10 50]	[231.15 235.15]	n/a	n/a
Mossop (1955)	530 ⁺	238.65 ^a	[220 840]	[238.65 242.15]	0.5K/ min	0.2
Carte (1956)	15 ⁺	236.25 ^a	[10 20]	[235.15 237.15]	1K/min	0.2
	231.3 ^d	238.45 ^b	n/a	n/a	0.5K/min	0.2
	279.4 ^d	238.55 ^b	n/a	n/a	0.5K/min	0.2
	292.9 ^d	238.35 ^b	n/a	n/a	0.5K/min	0.2
	321.9 ^d	238.45 ^b	n/a	n/a	0.5K/min	0.2
	362.2 ^d	238.55 ^b	n/a	n/a	0.5K/min	0.2
	427.3 ^d	238.65 ^b	n/a	n/a	0.5K/min	0.2
	469.7 ^d	238.55 ^b	n/a	n/a	0.5K/min	0.2
	498.2 ^d	238.95 ^b	n/a	n/a	0.5K/min	0.2
	567.3 ^d	238.95 ^b	n/a	n/a	0.5K/min	0.2
	623.6 ^d	238.85 ^b	n/a	n/a	0.5K/min	0.2
	718.5 ^d	238.85 ^b	n/a	n/a	0.5K/min	0.2
	818.1 ^d	238.95 ^b	n/a	n/a	0.5K/min	0.2
	965.2 ^d	239.15 ^b	n/a	n/a	0.5K/min	0.2
	1179.8 ^d	239.45 ^b	n/a	n/a	0.5K/min	0.2
1408.4 ^d	239.65 ^b	n/a	n/a	0.5K/min	0.2	
Langham and Mason (1958)	66.1 ^d	237.35 ^a	n/a	n/a	0.33K/min	n/a
	92.3 ^d	237.65 ^a	n/a	n/a	0.33K/min	n/a
	115.3 ^d	238.15 ^a	n/a	n/a	0.33K/min	n/a
	144 ^d	238.25 ^a	n/a	n/a	0.33K/min	n/a
	171.8 ^d	238.15 ^a	n/a	n/a	0.33K/min	n/a
	270.5 ^d	238.55 ^a	n/a	n/a	0.33K/min	n/a
Hoffer (1961)	110 ⁺	236.55 ^a	[100 120]	[235.65 238.15]	1K/min	0.5
	130 ⁺	237.25 ^a	[125 145]	[235.65 238.15]	1K/min	0.5
Kuhns and Mason (1967)	1 ^d	233.05 ^a	n/a	n/a	6K/min	0.1
	5 ^d	234.65 ^a	n/a	n/a	6K/min	0.1
	8 ^d	235.15 ^a	n/a	n/a	6K/min	0.1
	10 ^d	235.45 ^a	n/a	n/a	6K/min	0.1
	20 ^d	236.15 ^a	n/a	n/a	6K/min	0.1
	30 ^d	236.75 ^a	n/a	n/a	6K/min	0.1

	40 ^d	237.05 ^a	n/a	n/a	6K/min	0.1
	50 ^d	237.25 ^a	n/a	n/a	6K/min	0.1
	60 ^d	237.35 ^a	n/a	n/a	6K/min	0.1
	70 ^d	237.45 ^a	n/a	n/a	6K/min	0.1
	80 ^d	237.55 ^a	n/a	n/a	6K/min	0.1
	90 ^d	237.65 ^a	n/a	n/a	6K/min	0.1
	100 ^d	237.65 ^a	n/a	n/a	6K/min	0.1
	120 ^d	237.65 ^a	n/a	n/a	6K/min	0.1
Broto and Clausse (1976)	3 ^d	234.35 ^a	n/a	n/a	1.25K/min	0.5
Cziczo and Abbatt (1999)	0.35 ^d	234.15 ^d	n/a	n/a	n/a	n/a
Bertram et al. (2000)	8.3 ⁺	235 ^a	[5.6 11.0]	n/a	10k/min	1.5
Prenni et al. (2001)	0.6 ⁺	234.95 ^d	n/a	n/a	1K/increment	0.2
Larson and Swanson (2006)	40 ⁺	237.15 ^a	[30 50]	n/a	n/a	n/a
Stan et al. (2009)	80 ^d	236.25 ^a	n/a	[235.35 237.15]	2~100K/sec	0.21
Earle et al. (2010)	2 ⁺	236.35 ^a	[0.8 4]	[236 236.75]	n/a	n/a
	3.4 ⁺	236.35 ^a	[1.2 10]	[236 236.75]	n/a	n/a
	5.8 ⁺	236.15 ^a	[2 14]	[235.5 236.75]	n/a	n/a
Murray et al. (2010)	25 ⁺	236.25 ^a	[10 40]	[235.9 236.7]	2.5K/min	0.6
	25 ⁺	236.05 ^a	[10 40]	[234.75 237.75]	5K/min	0.6
	25 ⁺	235.75 ^a	[10 40]	[236.45 237.75]	7.5K/min	0.6
	25 ⁺	235.51 ^a	[10 40]	[234.45 237.75]	10K/min	0.6
Riechers et al. (2013)	53 ^m	236.65 ^c	[35 71]	[236.55 237.44]	1K/min	0.3
	63 ^m	236.65 ^c	[33 93]	[236.49 237.5]	1K/min	0.3
	82 ^m	236.85 ^c	[58 106]	[236.67 237.63]	1K/min	0.3
	85 ^m	237.15 ^c	[67 103]	[236.93 237.77]	1K/min	0.3
	96 ^m	237.35 ^c	[63 129]	[236.89 237.91]	1K/min	0.3

621 Table 1. Information regarding the details of the homogeneous ice nucleation
622 experiments used in the comparison, including the size, the freezing temperature, as
623 well as the cooling rate and uncertainty of the experiments. Homogeneous freezing
624 temperature T_f , <a>: freezing temperature when half of the water droplets freezing
625 $T_{50\%}$, : freezing temperature when 95% of the water droplets freezing $T_{95\%}$, <c>:
626 freezing temperature when most of the droplets freezing (peak signal) T_{Mode} , and <d>:
627 not defined or provided by the experiments. Diameter of water droplets used in the
628 experiments, <+> median size, <m> mean size, and <d> not provided by the

629 experiments.

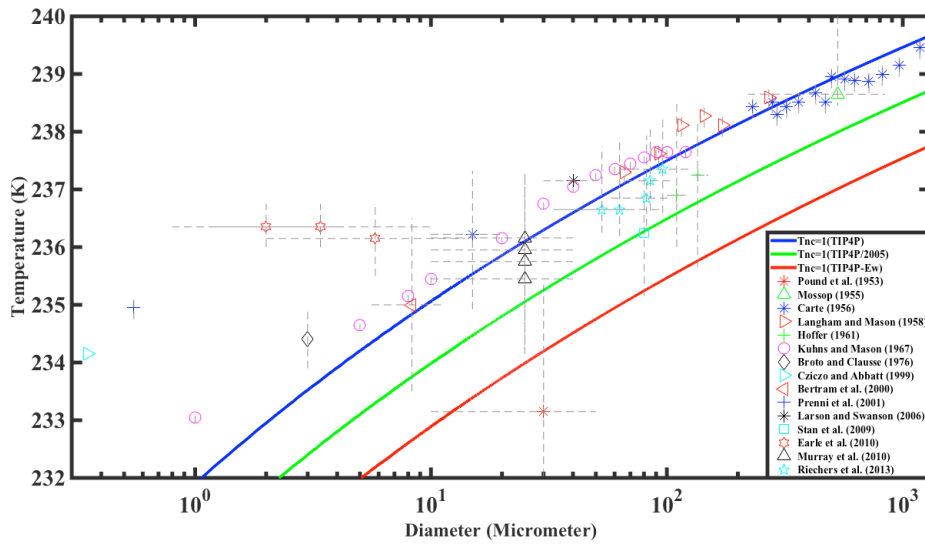
630

Diameter $\mu\pm\sigma$	96±11(μm)		85±6 (μm)		82±8 (μm)	
	Experiment values (K)	$T_{N_c=1}$ (K)	Experiment values (K)	$T_{N_c=1}$ (K)	Experiment values (K)	$T_{N_c=1}$ (K)
T_f^{onset}	237.91± 0.2	237.74	237.77± 0.2	237.53	237.63± 0.2	237.55
$T_f^{10\%}$	237.87± 0.2	237.59	237.76± 0.2	237.43	237.63± 0.2	237.42
$T_f^{50\%}$	237.4± 0.3	237.46	237.28± 0.3	237.34	237.13± 0.3	237.31
$T_f^{90\%}$	236.89± 0.3	237.31	236.93± 0.3	237.25	236.67± 0.3	237.18
T_f^{end}	N/A	237.05	N/A	237.11	N/A	236.97
Diameter $\mu\pm\sigma$	63±10 (μm)		53±6 (μm)			
	Experiment values (K)	$T_{N_c=1}$ (K)	Experiment values (K)	$T_{N_c=1}$ (K)		
T_f^{onset}	237.50± 0.2	237.43	237.44± 0.2	237.17		
$T_f^{10\%}$	237.46± 0.2	237.23	237.40± 0.2	237.02		
$T_f^{50\%}$	236.94± 0.3	237.05	236.94± 0.3	236.88		
$T_f^{90\%}$	236.49± 0.3	236.83	236.55± 0.3	236.72		
T_f^{end}	N/A	236.4	N/A	236.46		

631 Table 2. Comparison between the experimental results of the fraction experiment

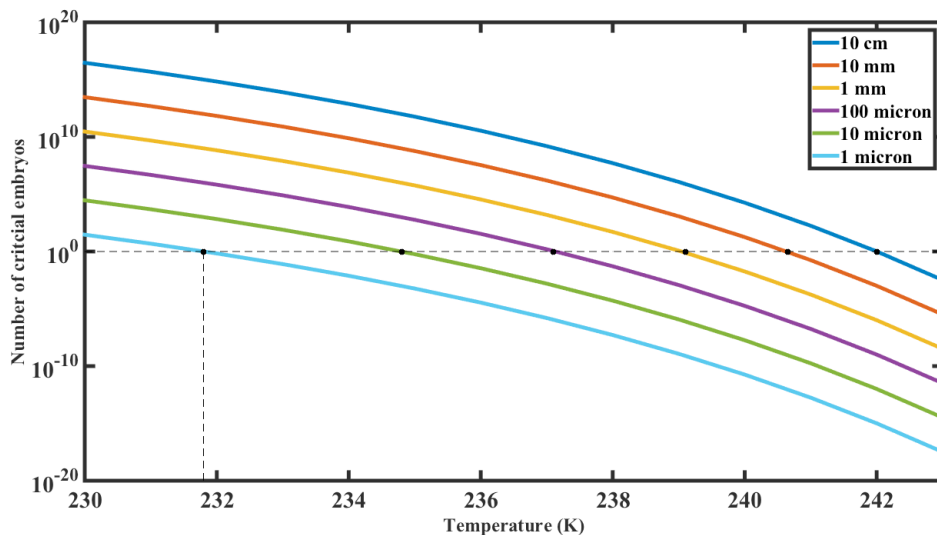
632 from Riechers et al. (2013) and the theoretical estimates $T_{N_c=1}$ derived here.

633



634

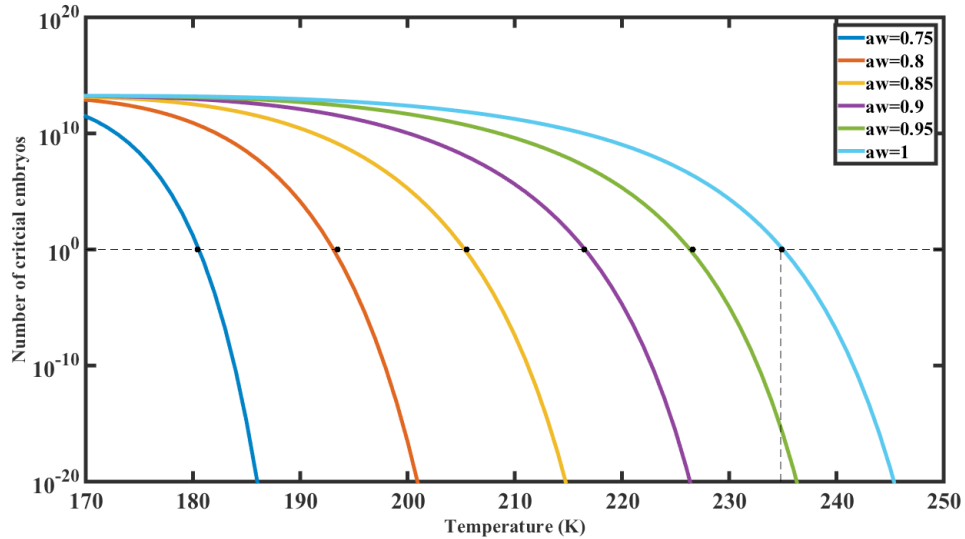
635 Figure 1. Freezing temperatures of pure water droplets: comparison between the
 636 approximations $T_{N_c=1}(V, a_w = 1)$ and the collected experimental data. Experimental
 637 data: the uncertainties and ranges of the drop size and the freezing temperatures are
 638 presented by the dotted line if information is provided by the studies (details in Table
 639 1). The approximations $T_{N_c=1}(V, a_w = 1)$: blue line - $\sigma_{i/w,e}$ from TIP4P model, green
 640 line - $\sigma_{i/w,e}$ from TIP4P/2005 model and red line - $\sigma_{i/w,e}$ from TIP4P- Ew model.



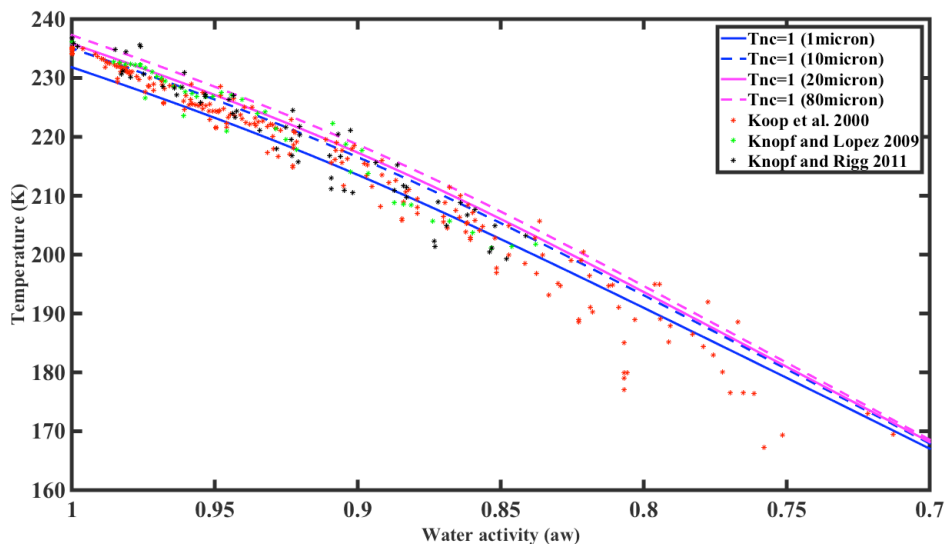
641

642 Figure 2. Mean number of critical embryos N_{c_mean} (by Eq. (1)) in a pure water
 643 droplet ($a_w = 1$) with different size (diameter) as a function of temperature. Solid

644 circle: the approximations $T_{N_c=1}(V, a_w)$ derived by Eq. (2) (using $\sigma_{i/w,e}$ from TIP4P
 645 model).

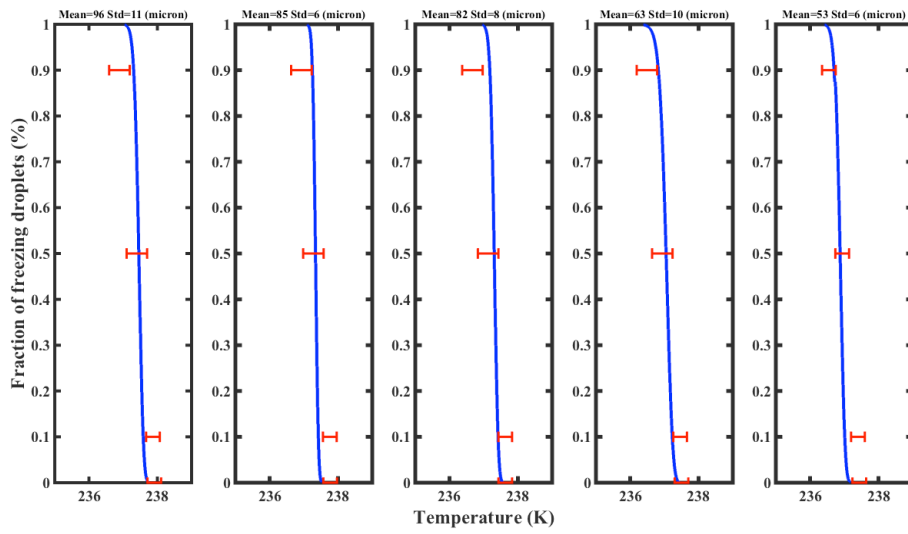


646
 647 Figure 3. Mean number of critical embryos N_{c_mean} (by Eq. (1)) in a solution droplet
 648 (diameter=1 μ m) with different water activity as a function of temperature. Solid circle:
 649 the approximations $T_{N_c=1}(V, a_w)$ derived by Eq. (2) (using $\sigma_{i/w,e}$ from TIP4P
 650 model).



651
 652 Figure 4. Comparison between the experimental data of freezing temperatures of
 653 solution droplets (Koop et al., 2000; Knopf and Lopez, 2009; Knopf and Rigg, 2011)

654 and the approximation $T_{N_c=1}(V, a_w)$.



655

656 Figure 5. Comparison between the experimental results of the fraction experiment

657 from Riechers et al. (2013) and the theoretical estimates derived here. Red:

658 experimental results with uncertainties from Riechers et al. (2013). Blue: theoretical

659 estimates ($\sigma_{i/w,e}$ from TIP4P model).

660